ACS Sustainable Chemistry & Engineering

Research Article

Cite This: ACS Sustainable Chem. Eng. 2018, 6, 12187−12196

pubs.acs.org/journal/ascecg

Smart Fertilization Based on Sulfur−Phosphate Composites: Synergy among Materials in a Structure with Multiple Fertilization Roles

Gelton G. F. Guimarães,[†,#] Rodrigo Klaic,[†,‡] Amanda S. Giroto,[†,§] Vinicius F. Majaron,[†,§] Waldir Avansi, Jr.,[∥] Cristiane S. Farinas,[†,‡] and Caue Ribeiro*[,†]

[†]Embrapa Instrumentation, Rua XV de Novembro, 1452, C.P. 741, São Carlos, Sao Paulo 13560-970, Brazil

[‡]Graduate Program of Chemical Engineering, [§]Department of Chemistry, and [∥]Department of Physics, Federal University of São Carlos, Rodovia Washington Luiz, km 235, São Carlos, São Paulo 13565-905, Brazil

Supporting Information

ABSTRACT: Sulfur is currently a bottleneck for agronomic productivity. Many products are based on the application of elemental sulfur (S°), but the ability of the soil to oxidize them is variable and dependent on the presence of oxidizing microorganisms. In this work, a composite was designed based on a matrix of S° prepared by low-temperature extrusion, reinforced by rock phosphate particles acting as P fertilizer, and with encapsulation of *Aspergillus niger* as an oxidizing microorganism. This structure was shown to be effective in significantly increasing S° oxidation while providing P by rock phosphate dissolution in an acid environment. X-ray absorption near-edge structure (XANES) spectra provided information about P fixation in the soil after dissolution, showing that the composite structure with *A. niger* modified the nutrient dynamics in the soil. This fully integrated material (a smart fertilizer) is an innovative strategy for eco-friendly agronomic practices, providing high nutrient delivery with minimal source preprocessing.

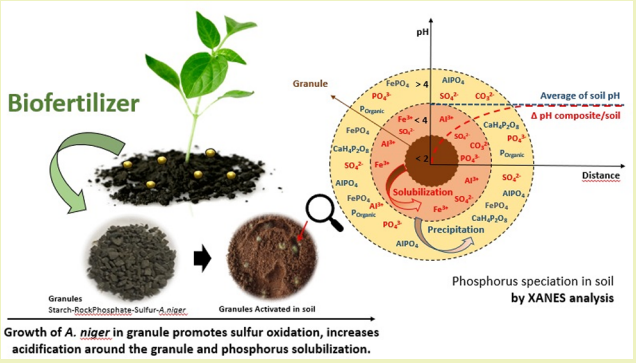

Growth of *A. niger* in granule promotes sulfur oxidation, increases acidification around the granule and phosphorus solubilization.

KEYWORDS: *Fertilizer, Phosphorus solubilization, Sulfur oxidation, Aspergillus niger, P speciation, XANES spectroscopy*

INTRODUCTION

Soil sulfur deficiency has increased in the last decades and provided a decrease in agronomic productivity. Recently, considerable attention has been given to studying new fertilizers based on N and S sources processed with multinutrients compounds.[1,2] The majority of fertilizer used in agriculture does not provide SO_4^{2-}, which is the actual nutrient absorbed by plants.[3,4] Many products are based on the application of elemental sulfur (S°), which is cheap and widely available, but the ability of the soil to oxidize them is variable and depends on the presence of oxidizing microorganisms,[5] besides soil physical and chemical characteristics, soil moisture and temperature, and particle size of S°.[6] Hence, the development of systems containing oxidizing microorganisms offers a way to ensure efficient oxidation of S°. Research has shown that the bacterium *Acidithiobacillus thiooxidans* can provide efficient S° oxidation,[7] but its low resistance to processing conditions and low inoculation viability reduces the availability of the microorganism. The filamentous fungus *Aspergillus niger* also has the ability to oxidize sulfur,[7−9] besides having a high capacity for the production of beneficial organic acids such as citric acid, oxalic acid, and gluconic acid, among others.[10]

However, incorporation of the spores of the microorganism in fertilizers on a large scale is still a challenge. Granular sulfur is used for direct spreading, but its production process leads to highly fragile materials that are very liable to powder formation, present low efficiency, and are difficult to inoculate. In order to overcome these problems, in this work a composite was designed based on a matrix of S° prepared by low-temperature extrusion, reinforced with nanoparticles with a fertilizer role, and encapsulation of *A. niger* to catalyze the S° oxidation process and P solubilization. Mineral apatites are highly suitable for this purpose, since P is also an essential element. Although mineral phosphates do not provide readily available P to plants,[11] their nanoparticles have increased solubility.[12] The dispersion of apatites in the matrix also avoids agglomeration, hence maintaining the higher solubility associated with the nanometric size.[13,14] The acidification provided by S° oxidation can solubilize the mineral phosphates,[15,16] in addition to the natural acidification caused by the production of organic acids by *A. niger*.[12,17] The organic acids lead to acidification of the medium and consequently provide increased phosphorus solubilization.[9,13] Only the simple mix of the S° with rock phosphates applied to the soil has not increased P solubility.[16,18,19]

Received: May 30, 2018
Revised: July 11, 2018
Published: July 22, 2018

DOI: 10.1021/acssuschemeng.8b02511
ACS Sustainable Chem. Eng. 2018, 6, 12187−12196

Table 1. Proportions of Starch (St), Rock Phosphate (RP), Elemental Sulfur (S°), and *A. niger* Spores (per g of total composite) Used in the Composites[a]

fertilizers	St (%)	RP (%)	S° (%)	RP/S° (%)	spores (per g)	P_2O_5 (%)	S (%)	Ca (%)
single superphosphate (SSP)						23.0	8.0	18.0
rock phosphate (RP)						32.0	0.6	48.3
elemental sulfur (S°)							95.0	
composite (RP/S°)		50.0	50.0			7.3	78.8	12.0
composite (St/RP)*	33.3	66.7			2×10^7	21.3	0.4	32.1
composite (St/S°)*	33.3		66.7		2×10^7		63.2	
composite (St/RP/S°)*	33.3			66.7	2×10^7	4.8	52.4	8.0

[a]Total contents of P_2O_5, S, and Ca determined by X-ray fluorescence analysis of single superphosphate (SSP), RP, S°, and the composites. Asterisks indicate samples with *A. niger* spores.

Thus, *A. niger* presents two mechanisms that may favor the P solubilization: first, by natural acidification provide S° oxidation and the second by organic acids production. Previous works evaluated strategies of isolated form to increase solubilization of phosphorus and did not evaluate the dynamics of P after its release in the soil.

Furthermore, the use of starch as a processing additive can provide a carbon source to support microorganism growth. The resulting fully integrated material (a smart fertilizer) offers an innovative strategy for eco-friendly agronomic practices, offering high nutrient delivery and minimal source preprocessing.

MATERIALS AND METHODS

Microorganism. The filamentous fungus *Aspergillus niger* C was obtained from the Embrapa Food Technology collection (Rio de Janeiro, RJ, Brazil). This organism was previously selected for rock phosphate solubilization by Klaic et al.[12] Fungal spore suspensions were kept at −18 °C and activated by incubation on Petri dishes containing potato dextrose agar for 96 h at 30 °C. After activation, spores were collected by adding distilled water, and a suspension of spores was obtained. The spore concentrations were determined using a Neubauer chamber.

Production of Composites. Sulfur (Sigma-Aldrich, St. Louis, MO) (size < 150 μm), rock phosphate (RP) from Patos de Minas (Vale Fertilizantes, SP, Brazil), corn starch (Amidex 3001, Ingredion, IL, USA), and urea (Synth, São Paulo, Brazil) were all used as received. As a reference, comparative experiments were performed using single superphosphate (SSP), since this commercial fertilizer is based on mineral phosphate phases with some sulfur content. The phosphate minerals were received premilled, with a particle size of around 256 nm. Physico-chemical characterization of the RP is available in the Supporting Information (Table S1).

First, the materials were prehomogenized using a 1:1 ratio of RP (50%) and sulfur (50%), followed by melt mixing using a torque rheometer (Rheodrive Rheomix OS4 mixer, Polylab) operated at 60 rpm for 10 min at 120 °C. After air drying, the samples were ground to below 500 μm prior to further incorporation (composite RP/S°). Sulfur (S°), RP, or composite RP/S°, in different proportions, was added to a gel of corn starch dispersed in water (10 wt %) and gelatinized at 90 °C, as described by Giroto et al.,[20] with mechanical stirring (model 713DS, Fisatom) at 3000 rpm for 5 min, followed by cooling to 30 °C for the incorporation of *A. niger* spores (1.2×10^7 spores per gram of the material) (composites St/RP, St/S° and St/RP/S°). The samples were dried at 50 °C with air circulation (model MA035/2, Marconi), ground to below 500 μm, and stored in dryboxes. All of the materials studied are summarized in Table 1.

The morphologies of the samples were analyzed by scanning electron microscopy (SEM). X-ray tomography was employed to analyze the granule homogeneity and microstructure. Details concerning sample characterization and the properties of the raw materials are provided in the Supporting Information.

Kinetics of SO_4^{2-} and PO_4^{3-} Release. The release of phosphorus from SSP, RP, and the composites (RP/S°, St/RP, and St/RP/S°) was evaluated using citric acid solution (20 g L^{-1}).[21] Portions of 0.5 g of each source, in triplicate, were placed in 50 mL volumes of the 2% citric acid solution in 125 mL Erlenmeyer flasks and kept in a constant temperature room at 25 °C. The samples were agitated for 30 min at 120 rpm using an orbital shaker, and the suspensions were then filtered through C 42 filter paper (Unifil, Germany) prior to determination of soluble P.

An incubation experiment (using submerged fermentation) was performed to measure the potential of *A. niger* for sulfur oxidation and phosphorus solubilization in a liquid nutrient medium (Czapek Dox) with initial pH 7, as proposed by Grayston et al.[8] The cultivation experiments were performed in 250 mL Erlenmeyer flasks, adding 50 mL of the nutrient medium to supply the minimal conditions required for spore germination and fungal growth. The experiments were standardized so that the P contents were the same (200 mg L^{-1}) as RP, RP/S°, St/RP, and St/RP/S°. For all samples, besides S° and St/S° composite, the concentration of S added to the culture medium was approximately 5000 mg L^{-1}. The incubation was carried out with independent samples for 3, 6, 9, and 12 days using an orbital shaker incubator at 30 °C and 220 rpm in triplicate. After each period the resulting material was vacuum filtered using Whatman No. 1 filter paper and centrifuged for 15 min at 11 000 rpm and 20 °C. The clear supernatant was analyzed to determine the SO_4^{2-} derived from S° oxidation, as well as soluble phosphorus. The SO_4^{2-} content was expressed as a percentage of the total S°, and the available P was expressed as a percentage of the total P added to the liquid medium. The methods for determination of sulfate and phosphorus were based on standard procedures.[22−24] The experimental steps are detailed in the Supporting Information.

Soil Experiments: Sulfur Oxidation and Phosphorus Solubilization. The oxidation of S° and solubilization of P were evaluated in a soil incubation experiment after incorporation of the composite samples in an Oxisol collected from the surface layer (0−20 cm) of an agricultural soil in the region of São Carlos in São Paulo State, Brazil, which was characterized according to its physical and chemical aspects.[25−27] Details of the soil characteristics are provided in the Supporting Information (Table S2).

To compare S° oxidation and P solubilization from RP in soil, triplicates of 50 g samples of soil were placed in 100 mL polyethylene screw-cap bottles. Addition was made of 10 mg of P as single superphosphate (SSP), rock phosphate (RP), or the RP/S°, St/RP, and St/RP/S° composites. Sulfur was added in the form of 100 mg of S° or St/S° composite. After complete incorporation of the fertilizers in the soil, the moisture content was adjusted to 80% of water holding capacity (WHC) using distilled water. The samples were monitored in independent units for each period before incubation (day 0) and after 30 and 60 days of keeping the bottles at a constant temperature of 25 °C under aerobic conditions. The water content was kept constant during the incubation. After each incubation period, the total soil sample was air dried and then crushed to pass through a 2 mm screen. The pH was determined as proposed by Embrapa,[26] and the exchangeable sulfate (SO_4^{2-}) was extracted using ammonium acetate solution.[24]

The available P was extracted with anionic resin using an anion exchange membrane (AMI 7001S, Membranes International Inc.,

DOI: 10.1021/acssuschemeng.8b02511
ACS Sustainable Chem. Eng. 2018, 6, 12187−12196

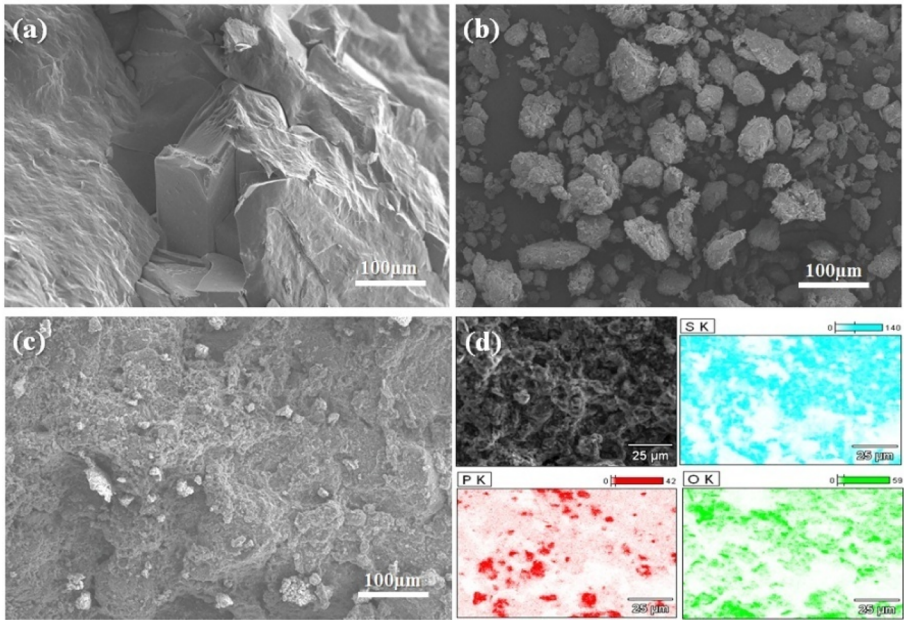

Figure 1. Scanning electron micrographs of (a) sulfur from the melt (S°), (b) rock phosphate (RP), and (c) the RP/S° composite. (d) Scanning electron micrograph and distribution of the elements S, P, and O in the RP/S° composite, obtained by EDX analysis.

Ringwood, NJ, USA).[28] Portions of 2.5 g of soil were placed in 50 mL polyethylene centrifuge tubes, together with 40 mL of distilled water and a 10 cm^2 AMI strip. The resulting suspensions were agitated for 16 h. The AMI strips were then removed from the tubes and washed to remove soil from the surfaces. The P absorbed by the AMI strip was extracted with 40 mL of 0.5 mol L^{-1} HCl under gentle agitation in an orbital shaker for 2 h.

Phosphorus Speciation in Soil. After incubation, the soil samples were analyzed using P K-edge X-ray absorption near-edge structure (XANES) at the soft X-ray spectroscopy (SXS) beamline of the Brazilian Synchrotron Light Laboratory (LNLS) in Campinas (São Paulo State, Brazil). The XANES data were collected in fluorescence mode in energy ranging between 2120 and 2250 eV with an energy step equal to 1.0 eV. In the region from 2149 to 2157 eV the energy step employed was equal to 0.2 eV. The analysis was performed by merging from 4 to 12 collected spectra with the spectra of all samples being normalized in the same conditions through Athena software.[29]

The phosphorus speciation in soil through XANES technique was performed with a similar procedure already reported.[30−34] In this way, the P distribution was analyzed in terms of the forms bonded to aluminum (P-Al), iron (P-Fe), calcium (P-Ca), and organic compounds (organic-P) using several mineralogical sources of these elements. The following reference materials were studied: hydroxyapatite ($Ca_5(PO_4)_3(OH)$), aluminum phosphate ($AlPO_4$), iron phosphate ($FePO_4$), calcium phosphate ($Ca_3(PO_4)_2$), phytic acid, lecithin, and three adsorbed phosphate samples (phosphate adsorbed on gibbsite (P-Al), goethite (P-Fe), and hematite (P-Fe)). The contribution of each species to the total P (P-Total) was estimated by linear combination fitting (LCF) in the energy range from −10 to 30 eV, performed with the Athena software.[29] First, several combinations of the reference compounds were tested, and based on previous results, the combination with the lowest *R* factors was selected. For this analysis, the control soil (without P fertilization and before incubation) and soil samples (composed of three replicates) from each treatment, after 30 and 60 days of incubation, were ground in an agate mortar.

RESULTS AND DISCUSSION

Characterization of the Materials. Table 1 shows the nutrient concentrations for all of the fertilizers and composites with the relative amounts of the raw materials and the effective nutrient values. Despite the low reactivity of RP, due to its igneous origin, it presented higher concentrations of P and Ca than the soluble commercial fertilizer used as a reference (SSP). The composites showed higher concentrations of S° and lower concentrations of P and Ca compared to SSP due to the elevated concentration of elemental sulfur. Significant concentrations of P and Ca were observed for the materials obtained only by combination of RP and S°.

The SEM images of S° (recrystallized from the melt) and RP are shown in Figure 1. The sulfur particles (Figure 1a) presented large and dense structures after melting, while the RP particles presented heterogeneous granulometry after grinding (Figure 1b), probably due to reclumping of the particles, but still with agglomerate diameters smaller than 100 μm. The RP/S° composite (Figure 1c) exhibited a homogeneous dispersion of RP particles in the S° matrix, as indicated by the elemental distribution in the composite (Figure 1d). Figure 1d also presents the energy-dispersive X-ray spectroscopy (EDS) analysis of a selected region, with P points distributed across the composite surface. Strong P points were due to agglomerated RP particles, but nonetheless, a homogeneous distribution was maintained in the S° matrix.

Figure 2 presents the X-ray tomography cross-sectional images of the composites after the encapsulation of RP/S° in the starch matrix. The encapsulation of the particles of S°, RP, and the RP/S° composite in the starch matrix can be identified by the color scale distribution, which corresponds to the density of the material. No agglomeration effects were observed for any of the composites. It can be seen that there was good dispersion of S° in the starch matrix, characterized as dense material due to the higher homogeneity among starch and sulfur (Figure 2c). Figure 2d−f shows micrographs of the surface structures, indicating that (as shown by the microtomography) the starch matrix was compatible with all of the materials, avoiding agglomerated parts. Figure 2f shows spheroid shapes with diameters larger than 12 μm on the surface of the composite, identified as *A. niger* spores. Hence, the starch matrix encapsulated the spores,

DOI: 10.1021/acssuschemeng.8b02511
ACS Sustainable Chem. Eng. 2018, 6, 12187−12196

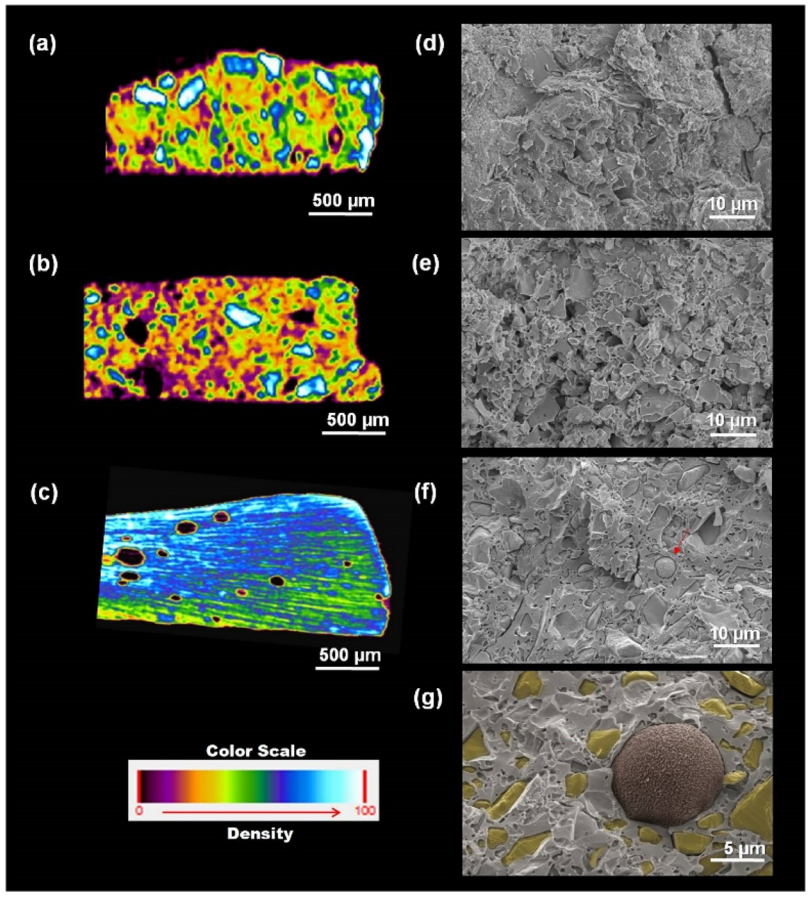

Figure 2. X-ray tomography cross-sectional images of the composites (a) St/RP, (b) St/RP/S°, and (c) St/S°. SEM images of (d) St/RP, (e) St/RP/S°, and (f) St/S°. (g) Magnified SEM image of the St/S° composite, showing S° crystals (yellow) and an *A. niger* spore (brown) in the structure.

protecting them against possible changes occurring in the environment. In addition, the encapsulation maintained the spores viable for a longer period, allowing them to be activated when incorporated into the culture medium or moist soil.

Phosphorus Release in Citric Acid Solution. The results for phosphorus solubilization in citric acid solution (Figure 3) showed that dispersion of the RP particles in the S°

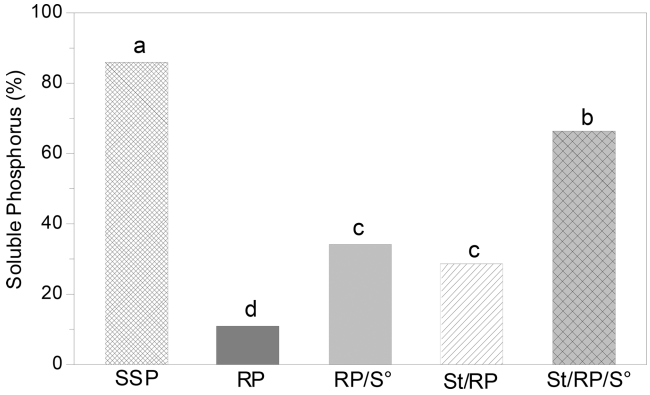

Figure 3. Phosphorus release from single superphosphate (SSP), rock phosphate (RP), and composites RP/S°, St/RP, and St/RP/S° in 2% citric acid solution. Different letters indicate significant difference between the treatments (ANOVA with Tukey's test, 95% confidence level).

matrix (RP/S° composite) or in the starch matrix (St/RP composite) acted to increase the solubility of P by around 3-fold compared to the original RP. This behavior can also be seen for the St/RP/S° composite (RP dispersed first in the S° matrix, followed by encapsulation in starch) with solubilization of around 60% of the total P applied, which was 6-fold higher than for pristine RP. This was consistent with the findings of Giroto et al.[13,14] for dispersions of hydroxyapatite powders.

Phosphorus Solubilization and Sulfur Oxidation in Submerged Fermentation. An initial set of experiments was carried out to analyze the potential of *A. niger* for sulfur oxidation, consequently leading to phosphorus solubilization. Figure 4a shows the P solubilization and pH during the incubation period under submerged cultivation for the St/RP and St/RP/S° composites as well as the solubilization of RP (control) and RP/S° without *A. niger* spores. The results demonstrated that the RP particles dispersion during processing of the St/RP and St/RP/S° composites and the bioactivation of the *A. niger* resulted in greater P solubilization (of around 30%) compared to the RP and RP/S° composites without spores (3−5%) after incubation for 3 days. This confirmed that use of the starch matrix was effective in keeping the encapsulated *A. niger* spores inactive and viable, only allowing fungal growth when the composites were placed under favorable environmental conditions (Supporting Information, Figure S1). In all cases, the spores remained viable after 30 days storage at room temperature, indicative of a considerable shelf life.

After incubation for 6 days, P solubilization from the St/RP/S° composite increased to around 85% of total available P, while the

DOI: 10.1021/acssuschemeng.8b02511
ACS Sustainable Chem. Eng. 2018, 6, 12187−12196

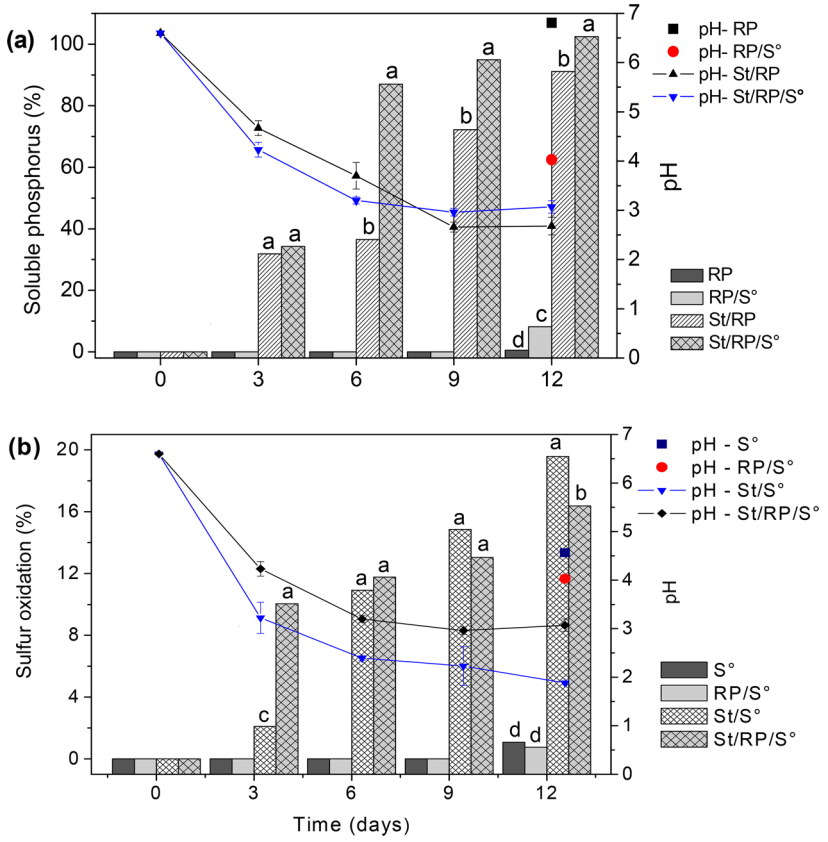

Figure 4. Temporal profiles of (a) phosphorus solubilization in culture medium and pH for treatments using RP (control, without *A. niger*) and the composites RP/S°, St/RP, and St/RP/S° and (b) elemental sulfur oxidation in culture medium and pH for treatments using S° (control, without *A. niger*) and the composites RP/S°, St/S°, and St/RP/S°. Different letters indicate significant difference between the treatments (ANOVA with Tukey's test, 95% confidence level).

St/RP composite showed P solubilization of 38% over the same period, evidencing the synergy among *A. niger* and S° in acidifying the medium. The solubilization of P continued to increase, reaching values of 100% and 90% for the St/RP/S° and St/RP composites, respectively, after 12 days of incubation. In the case of the materials without fungus, the RP/S° composite showed release of only 8% of the total available P, while for pure RP, the release was only 0.5%. Interestingly, the pH values of the samples were similar and remained almost the same (around pH 3) after incubation for 12 days, suggesting that the solubilization involved dynamic ion exchange (such as by the replacement of phosphate in the RP structure by organic anions). This showed that the solubilization was governed probably by the total amount of counterions available for phosphate release, which was not necessarily associated with variation in pH. In addition, the buffering capacity of the RP can also have affected the reduction of the pH during the incubation.

Therefore, solubilization of P from the St/RP/S° and St/RP composites was substantially higher than from the PR/S° and RP composites, evidencing that the inoculation of *A. niger* was responsible for increasing the solubilization. *A. niger* by itself promoted acidification of the medium due to the production of organic acids such as citric, oxalic, gluconic, malic, succinic, and tartaric acids, among others, as also observed by Li et al.[38] (Supporting Information, Figure S1). These acids can form complexes with calcium, iron, aluminum, and other metals present in the structure of the phosphate material, hence releasing phosphate groups to the medium. This has been reported as the main mechanism for solubilization of inorganic phosphate by microorganisms. However, other studies have shown that *A. niger* can also promote the oxidation of sulfur to sulfate.[7] This process acidifies the medium and also results in increased P solubilization, as evidenced by the higher solubilization of P from the St/RP/S° composite compared to the composite without S° (St/RP). In order to obtain a better understanding of the effect of sulfur oxidation on phosphorus solubilization, the oxidation of S° (Figure 4b) was monitored simultaneously with the total acidity from the organic acids produced by *A. niger* (Supporting Information, Figure S2).

Figure 4b shows the S° oxidation for all of the composites and for the S° control (without *A. niger*). The St/RP/S° composite showed oxidation of around 10% of the initial S° in 3 days, while the St/S° composite showed oxidation of only 2%. No oxidation signals were observed for the other composites. However, after 12 days, the St/S° and St/RP/S° composites showed increases of S° oxidation to 20% and 16%, respectively. It should be noted that in these experiments it was decided to use very high S° contents in order to reveal the effects associated with the structure of the composite (including the action of the microorganism). Therefore, the data corresponded to oxidation levels exceeding 40 mg S°, providing high SO_4^{2-} concentrations in the culture medium (above 800 mg L^{-1}). In contrast, the RP/S° composite and S° presented oxidation of only 0.7% and 1%, respectively, without any microorganism present. These results confirmed the role of *A. niger* in promoting the oxidation of S° to the sulfate form (SO_4^{2-}), as described by Grayston,[8] Li et al.,[9] and

DOI: 10.1021/acssuschemeng.8b02511
ACS Sustainable Chem. Eng. 2018, 6, 12187−12196

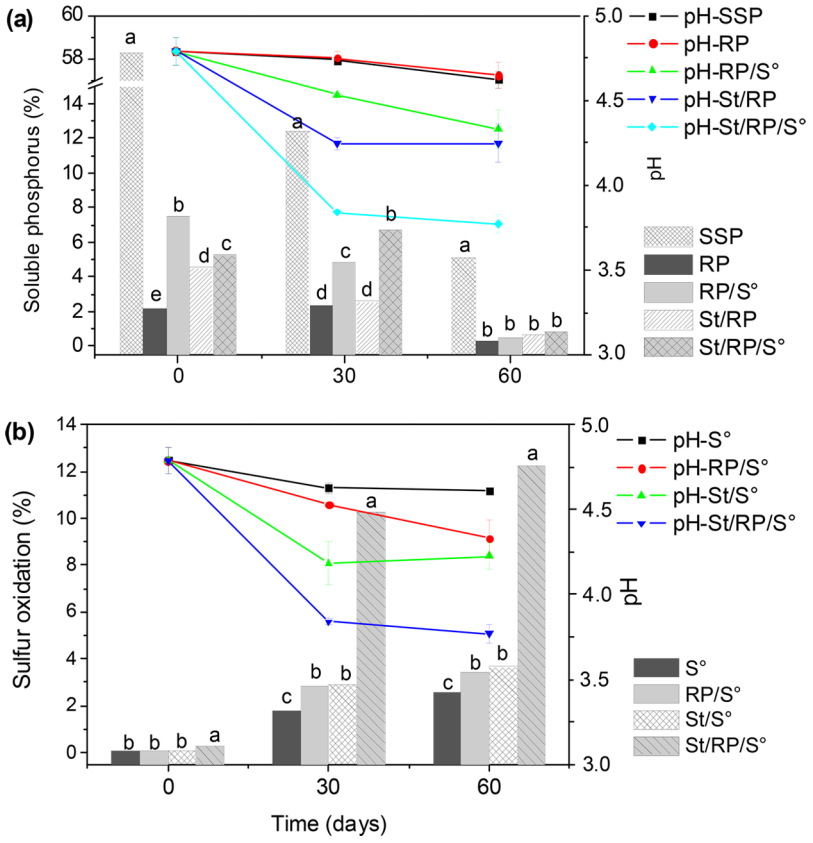

Figure 5. Temporal profiles of (a) phosphorus solubilization in soil and pH for treatments using SSP, RP (control, without *A. niger*), and the composites RP/S°, St/RP, and St/RP/S° and (b) elemental sulfur oxidation in soil and pH for treatments using S° (control, without *A. niger*) and the composites RP/S°, St/S°, and St/RP/S°. Different letters indicate significant difference between the treatments (ANOVA with Tukey's test, 95% confidence level).

Mattiello at al.[7] The increase in total acidity during the incubation experiments was directly related to the amount of sulfur oxidized (Supporting Information, Figure S1). Therefore, the greatest changes in total acidity were found for the composites that presented the highest S° oxidation rates. These results indicated that the highest P solubilization obtained for the St/RP/S° composite could be attributed to bioactivation of the composite, followed by S° oxidation and increased acidification.

Sulfur Oxidation and Phosphorus Solubilization in Soil Experiments. Figure 5a shows the results for P release from the composites and fertilizer incorporated in the soil at time zero and after 30 and 60 days of incubation. As expected, the single superphosphate fertilizer (SSP) presented high solubility in the soil, with 60% of P solubilized, relative to the total P applied. The RP/S°, St/RP, and St/RP/S° composites showed up to 3.4-fold increases of P solubilization, compared to RP, for the same incubation time. The increases could be attributed exclusively to the effect of dispersion, as evidenced by the release of P in citric acid, due to the absence of the natural acidification provided by *A. niger*. However, there was rapid fixation of P by the soil colloids during the incubation period, which for SSP reduced the availability of P in the soil to 12% after 30 days of incubation, while the St/RP/S° composite showed an increase in P solubilization from 5.2% to 6.7%. After 60 days of incubation, the availability of P from all of the composites became similar to that of RP. The reductions of the pH of the soils fertilized with the composites RP/S°, St/RP, and especially St/RP/S° were consistent with the expected action of *A. niger* in S° oxidation and organic acids production, as discussed in Phosphorus Solubilization and Sulfur Oxidation in Submerged Fermentation.

Nevertheless, it was not possible to analyze P solubilization without considering the immobilization of P by other mineral fractions. This effect, widely known as a major difficulty in phosphate fertilization, probably occurred during these experiments, since part of the released P was shown to be unavailable for extraction after the 30-day incubation, especially in the case of the soluble SSP source (Figure 5a). Therefore, S° oxidation and pH were monitored in the soil (Figure 5b). Compared to the S°, all of the composites showed greater oxidation of elemental sulfur. In the case of the St/RP/S° composite, there was oxidation of over 12% of the total S applied in the soil after 60 days of incubation, while oxidation of only 2.5% was obtained for the pristine S°, and the other composites showed oxidation of around 3.5% during the same period. The St/RP/S° treatment also presented a greater decrease of soil pH compared to the other treatments. The higher S° oxidation observed for the St/RP/S° composite, compared to the material containing only starch and sulfur (St/S°), could be explained by the presence of available nutrients such as P and Ca derived from the phosphate rock, which could have favored the growth and metabolism of *A. niger*.

Phosphorus Speciation in Soil. Although the previous experiments indicated that small fractions of P were available in the soil after 30 days of incubation, it is not clear if this was related to unreacted material (such as undissolved rock) or to further immobilization events associated with the kinetics of P in the soil. In recent years, several investigations have

DOI: 10.1021/acssuschemeng.8b02511
ACS Sustainable Chem. Eng. 2018, 6, 12187−12196

Table 2. Relative Distributions of Each P Species Obtained from XANES analyses in the Samples (mean of three replicates) of Single Superphosphate (SSP), Rock Phosphate (RP), Soil Control (without P fertilization), and Soil Fertilized with SSP, RP, RP/S°, and St/RP/S° after 30 or 60 Days of Incubation

samples	phytic acid (P-organic)	goethite (P-Fe)	hematite (P-Fe)	apatite (P-Ca)	FMC[a] (P-Ca)	gibbsite (P-Al)	factor *R*	pH[b]
single superphosphate (SSP)	0.138 (0.038)			0.380 (0.012)	0.482 (0.030)		0.006	
rock phosphate (RP)	0.017 (0.107)		0.060 (0.083)	0.923 (0.042)			0.002	
soil control	0.854 (0.053)	0.050 (0.037)			0.095 (0.099)		0.013	4.80
soil fertilized with SSP (30)	0.442 (0.055)				0.558 (0.051)		0.013	4.74
soil fertilized with SSP (60)	0.350 (0.063)				0.650 (0.060)		0.018	4.62
soil fertilized with RP (30)		0.158 (0.040)	0.675 (0.097)	0.167 (0.034)			0.023	4.75
soil fertilized with RP (60)	0.131 (0.068)	0.025 (0.025)	0.477 (0.046)		0.367 (0.043)		0.005	4.65
soil fertilized with RP/S° (30)	0.151 (0.049)		0.307 (0.111)		0.542 (0.077)		0.016	4.53
soil fertilized with RP/S° (60)	0.117 (0.027)		0.505 (0.080)		0.378 (0.042)		0.005	4.33
soil fertilized with St/RP (30)	0.276 (0.015)		0.173 (0.042)	0.219 (0.062)	0.333 (0.027)		0.001	4.25
soil fertilized with St/RP (60)	0.280 (0.027)		0.253 (0.074)	0.221(0.098)	0.246 (0.049)		0.005	4.37
soil fertilized with St/RP/S° (30)	0.588 (0.069)				0.412 (0.124)		0.023	3.84
soil fertilized with St/RP/S° (60)	0.042 (0.021)	0.051 (0.190)			0.171 (0.045)	0.736 (0.029)	0.004	3.77

[a]Monobasic calcium phosphate. [b]Soil pH after incubation.

demonstrated that P species in soil can be studied by X-ray absorption spectroscopy (XAS), especially in the XANES region, where the dominant species of P can be estimated using linear combination fitting (LCF).[30−37] To this, a weighted sum of XANES spectra from selected P standards are fit to the spectrum from a sample, since P K-edge XANES spectra for standard compounds provided clear spectral features in the pre-edge, white-line peak and postedge regions, which is important to identification of P species in the studied soil samples.[30−34] In order to properly assess the P species in the soil, analysis using the P K-edge XANES technique was performed to quantify the P fractions associated with aluminum (P−Al), iron (P-Fe), calcium (P-Ca), and organic compounds (P-organic) (Support Information, Figure S3). Figure S3a shows the profiles for P K-edge XANES spectra, chosen as representative standard compounds of the expected forms of phosphate immobilization. These included three P-containing phases (monobasic calcium phosphate (FMC), phytic acid, and hydroxyapatite) and three surface-immobilized P phases (P-goethite, P-gibbsite, and P-hematite). The XANES spectra for reference compounds present their typical features, in good agreement with the literature,[30−34] Figure S3a. Indeed, in Figure S3a it is possible to observe that XANES spectra for hydroxyapatite present a post-white-line shoulder at around 2155 eV, which has been attributed as an indication of Ca−P compounds, and the presence of a secondary post-white-line peak at 2164 eV, suggesting different degrees of crystallinity of the P compounds.[30−34] XANES spectra for P-absorbed solids including P adsorbed to gibbsite and ferrihydrite showed a more pronounced intensity of the white-line peak, which is considered as an indication of P-sorbed species compared to P minerals.[30−34] According to the literature, for organic P species any clear pre- or postedge features could be observed.[30−34]

Figure S3b shows the representative spectrum profiles for the samples incubated for 60 days. Table 2 summarizes the relative distributions of the immobilized P phases after incubation for 30 and 60 days compared to SSP, RP, and the soil (control) before incubation. The soil showed a P distribution with a predominance of P-organic "phytic acid" (85.5%) and low presence of P-goethite (5%) and FMC (9.5%) without significant immobilization in Al phases. The total P content of the soil before fertilization was very low (0.5 mg kg^{-1}) (Supporting Information, Table S2), suggesting that further P immobilization was associated with the added P. As expected, the results for SSP confirmed that this sample mainly consisted of the FMC phase. Nevertheless, smaller fractions of apatite (38%) and P-organic (14%, probably as a contaminant) were also observed. The RP was (unexpectedly) almost an apatite (hydroxy- or fluoroapatite), and there were no immobilized P fractions before the incubation.

After incubation for 30 days, the results for the soil fertilized with SSP indicated that a significant fraction of P (44%) was immobilized as phytic acid, reflecting the biological activity in the soil. This was in agreement with the results shown in Figure 5a, indicative of a substantial reduction of the total available P in this system. For the samples after 60 days of incubation, the system maintained the same characteristics with some reprecipitation of FMC but within statistical margins of error. However, the results for the soil fertilized with RP indicated that the apatite was solubilized in this time interval and reprecipitated mainly as P-hematite. This was a very important result, because it indicated that the high amount of Fe (6.92% by mass) (Supporting Information, Table S1) in the RP composition was the key parameter affecting P immobilization. Since the solubilization occurred closest to the iron mineral phase, the kinetics of P immobilization was very fast compared to SSP, as also seen in the P-goethite content. After 60 days of incubation, the immobilization as phytic acid increased, probably due to soil biological activity, but a significant amount of P immobilized in iron phases was still present, consistent with the results obtained for extractable P.

In the case of the composite materials, the immobilization of P was affected by the dynamics of soil acidulation. The soil fertilized with RP/S° showed a small pH reduction due to S° oxidation. This small reduction acted to reduce the immobilization of P in iron phases (compared to the soil fertilized only with RP), probably due to increased solubility of Ca in neighboring granules. According to Mendes et al.,[39] FMC and other Ca phases are fairly soluble at pH below 4.5. Therefore, higher Ca concentrations may increase FMC precipitation, as observed here, with precipitation values of 54% and 38% after 30 and 60 days, respectively. It should be noted that the measured pH corresponded to the average soil pH, rather than the local value at the granule surface. Small decreases were

DOI: 10.1021/acssuschemeng.8b02511
ACS Sustainable Chem. Eng. 2018, 6, 12187−12196

Scheme 1. Schematic View of SO_4^{2-} and PO_4^{3-} Evolution along the Soil Profile, According to the Distance from the Composite Surface and the Expected Local pH

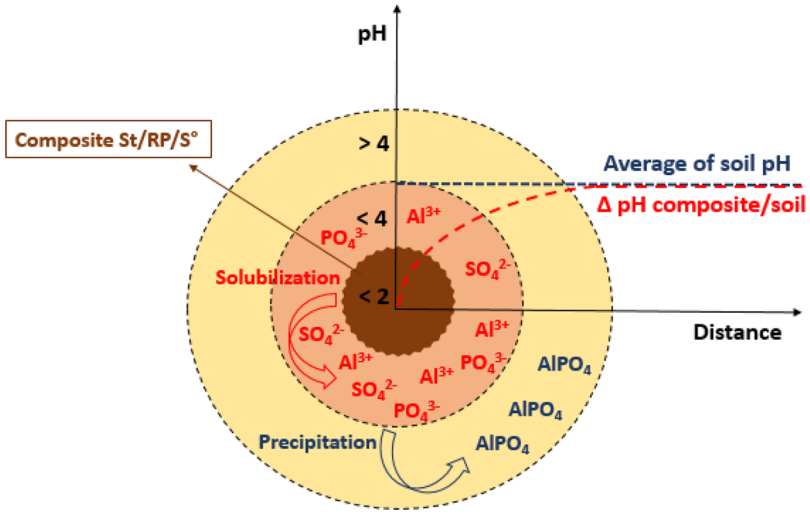

probably related to surface pH effects associated with the higher SO_4^{2-} contents in this system.

In the systems inoculated with *A. niger*, the production of organic acids led to higher phytic acid fractions. Organic acids such as citric and oxalic acids are good complexation agents for Ca and Fe, hence affecting the availability of Ca. The most remarkable result was found for the St/RP/S° system, where the material presented the same characteristics as RP/S° in terms of local acidulation but the higher SO_4^{2-} production led to a harsher pH, causing Al solubilization. According to the Pourbaix diagram[40] for Al, aluminum phases (including oxides) are highly soluble at pH < 4, with subsequent reprecipitation as P-Al phases. This probably occurred in a diffusion zone (Scheme 1) where the pH was reduced to the average soil pH and Al phases could reprecipitate. This is interesting to note since the Pourbaix diagram for Fe indicates that hematite should only be highly soluble at pH < 1, providing further evidence that P-hematite was not favored in this system. Concerning the uncertainty in XANES results, since the interpretation of the statistical parameters in the linear combination fit is considered a challenge, several papers reported consistent results based on this approach.[30−37] Indeed, the mean expected deviation reported for this protocol[35−37] does not have a significant difference in phosphate immobilization behaviors in each condition. Therefore, despite the fact that these results do not exclude the need of future pot and in-field trials for clear evidence of agronomic effects, XANES data give evidence that our composite strategy can positively affect the P availability, which is important for effective phosphate management.

CONCLUSIONS

A simple and viable method was developed to produce a composite consisting of a nutrient matrix (S°), with the structure formed by another nutrient source (rock phosphate), resulting in a multinutrient material. The inclusion of *A. niger* provided a means for improved S° oxidation and concomitant faster P release. The proposition of a granule fertilizer with a simultaneous dispersion of particles of phosphate rock, elemental sulfur, and *A. niger* spores can allow the reduction of preprocessing (e.g., for soluble fertilizer production) and reduces the indirect costs related to the conventional acid solubilization process and waste treatment. Soil incubation studies, probed by XANES, indicated that the composite structure played a role in nutrient fixation and immobilization, showing that nutrient dynamics was governed by the local pH. The immobilization was influenced by the other components of the mineral P source (especially Ca, Fe, and Al) rather than by the soil composition. The innovative concept of "granule bioreactor" fertilizer, where the microorganism grows in the granule after application in the soil, provides the S° oxidation and the P solubilization from *in nature* nutrient sources by an eco-friendly process. These results provide a background for a new generation of multifunctional smart fertilizers that provide better nutrient recovery by plants.

ASSOCIATED CONTENT

Supporting Information

The Supporting Information is available free of charge on the ACS Publications website at DOI: 10.1021/acssuschemeng.8b02511.

Chemical analysis by X-ray fluorescence for rock phosphate and particle size; chemical and physical properties of soil studied; image of the composites before incubation, composite activated in culture medium, and activated in soil; temporal profiles of the total acidity produced by composites; normalized P K-edge XANES spectra of mineral compounds used as standards and soil fertilized with composites after 60 days incubation (PDF)

AUTHOR INFORMATION

Corresponding Author

*E-mail: caue.ribeiro@embrapa.br. Phone: +55 16 2107 2915. Fax: +55 16 2107 2903.

Present Address

#(G.G.F.G.) EPAGRI - Agricultural Research and Rural Extension Company of Santa Catarina. 6800 Rd. Antônio Heil, Itajaí, Santa Catarina, 88318112, Brazil.

ORCID

Gelton G. F. Guimarães: 0000-0001-9029-5241

Cristiane S. Farinas: 0000-0002-9985-190X

Caue Ribeiro: 0000-0002-8908-6343

DOI: 10.1021/acssuschemeng.8b02511
ACS Sustainable Chem. Eng. 2018, 6, 12187−12196

Notes

The authors declare no competing financial interest.

■ ACKNOWLEDGMENTS

This work was supported by FAPESP (São Paulo State Research Foundation, grant nos. 22016/09343-6 and 2013/11821-5), CNPq (Brazilian National Council for Scientific and Technological Development, grant no. 142348/2014-7), and CAPES. XANES measurement facilities were provided by LNLS-Campinas, SP, Brazil (research proposal no. 20160386). We also thank the Agronano Network (Embrapa Research Network), the Agroenergy Laboratory, and the National Nanotechnology Laboratory for Agribusiness (LNNA) for support and facilities.

■ REFERENCES

(1) Baltrusaitis, J.; Sviklas, A. M.; Galeckiene, J. Liquid and solid compound granulated diurea sulfate-based fertilizers for sustainable sulfur source. *ACS Sustainable Chem. Eng.* **2014**, *2* (10), 2477−2487.
(2) Honer, K.; Kalfaoglu, E.; Pico, C.; McCann, J.; Baltrusaitis, J. Mechanosynthesis of magnesium and calcium salt urea ionic cocrystal fertilizer materials for improved nitrogen management. *ACS Sustainable Chem. Eng.* **2017**, *5* (10), 8546−8550.
(3) Scherer, H. W. Sulphur in crop production - invited paper. *Eur. J. Agron.* **2001**, *14* (2), 81−111.
(4) Degryse, F.; Ajiboye, B.; Baird, R.; da Silva, R. C.; McLaughlin, M. J. Oxidation of elemental sulfur in granular fertilizers depends on the soil-exposed surface area. *Soil Science Society of America Journal* **2016**, *80* (2), 294−305.
(5) Zhao, C. C.; Gupta, V.; Degryse, F.; McLaughlin, M. J. Abundance and diversity of sulphur-oxidising bacteria and their role in oxidising elemental sulphur in cropping soils. *Biol. Fertil. Soils* **2017**, *53* (2), 159−169.
(6) Attoe, O. J.; Olson, R. A. Factors affecting rate of oxidation in soils of elemental sulfur and that added in rock phosphate-sulfur fusions. *Soil Sci.* **1966**, *101* (4), 317.
(7) Mattiello, E. M.; da Silva, R. C.; Degryse, F.; Baird, R.; Gupta, V.; McLaughlin, M. J. Sulfur and zinc availability from co-granulated Zn-enriched elemental sulfur fertilizers. *J. Agric. Food Chem.* **2017**, *65* (6), 1108−1115.
(8) Grayston, S. J.; Nevell, W.; Wainwright, M. Sulfur oxidation by fungi. *Trans. Br. Mycol. Soc.* **1986**, *87*, 193−198.
(9) Li, X. S.; Sato, T.; Ooiwa, Y.; Kusumi, A.; Gu, J. D.; Katayama, Y. Oxidation of elemental sulfur by Fusarium solani strain THIF01 harboring endobacterium Bradyrhizobium sp. *Microb. Ecol.* **2010**, *60* (1), 96−104.
(10) Papagianni, M. Advances in citric acid fermentation by Aspergillus niger: biochemical aspects, membrane transport and modeling. *Biotechnol. Adv.* **2007**, *25* (3), 244−263.
(11) Valadares, R. V.; Cantarutti, R. B.; Mattiello, E. M.; Vieira, R. F. Agronomic effectiveness of rock phosphate combined with nitrogen sources in spot application: A pot experiment. *J. Plant Nutr. Soil Sci.* **2017**, *180* (5), 585−593.
(12) Klaic, R.; Plotegher, F.; Ribeiro, C.; Zangirolami, T. C.; Farinas, C. S. A novel combined mechanical-biological approach to improve rock phosphate solubilization. *Int. J. Miner. Process.* **2017**, *161*, 50−58.
(13) Giroto, A. S.; Guimarães, G. G. F.; Foschini, M.; Ribeiro, C. Role of slow-release nanocomposite fertilizers on nitrogen and phosphate availability in soil. *Sci. Rep.* **2017**, *7*, 11.
(14) Giroto, A. S.; Fidelis, S. C.; Ribeiro, C. Controlled release from hydroxyapatite nanoparticles incorporated into biodegradable, soluble host matrixes. *RSC Adv.* **2015**, *5* (126), 104179−104186.
(15) Ullah, I.; Jilani, G.; Khan, K. S.; Akhtar, M. S.; Rasheed, M. Sulfur oxidizing bacteria from sulfur rich ecologies exhibit high capability of phosphorous solubilization. *Int. J. Agric. Biol.* **2014**, *16* (3), 550−556.
(16) Rajan, S. S. S. Effect of sulfur-content of phosphate rock sulfur granules on the availability of phosphate to plants. *Fert. Res.* **1983**, *4* (3), 287−296.
(17) Mendes, G. D.; da Silva, N.; Anastacio, T. C.; Vassilev, N. B.; Ribeiro, J. I.; da Silva, I. R.; Costa, M. D. Optimization of Aspergillus niger rock phosphate solubilization in solid-state fermentation and use of the resulting product as a P fertilizer. *Microb. Biotechnol.* **2015**, *8* (6), 930−939.
(18) Evans, J.; McDonald, L.; Price, A. Application of reactive phosphate rock and sulphur fertilisers to enhance the availability of soil phosphate in organic farming. *Nutr. Cycling Agroecosyst.* **2006**, *75* (1−3), 233−246.
(19) Stanislawska-Glubiak, E.; Korzeniowska, J.; Hoffmann, J.; Gorecka, H.; Jozwiak, W.; Wisniewska, G. Effect of sulphur added to phosphate rock on solubility and phytoavailability of phosphorus. *Pol. J. Chem. Technol.* **2014**, *16* (1), 81−85.
(20) Giroto, A. S.; de Campos, A.; Pereira, E. I.; Cruz, C. C. T.; Marconcini, J. M.; Ribeiro, C. Study of a nanocomposite starch-clay for slow-release of herbicides: evidence of synergistic effects between the biodegradable matrix and exfoliated clay on herbicide release control. *J. Appl. Polym. Sci.* **2014**, *131* (23), 9.
(21) *Manual de métodos analíticos oficiais para fertilizantes e corretivos*; Ministério da Agricultura Pecuária e Abastecimento (MAPA): Brasília, 2014; p 220.
(22) Murphy, J.; Riley, J. P. A modified single solution method for the determination of phosphate in natural waters. *Anal. Chim. Acta* **1962**, *27*, 31−36.
(23) Drummond, L.; Maher, W. Determination of phosphorus in aqueous-solution via formation of the phosphoantimonylmolybdenum blue complex - reexamination of optimum conditions for the analysis of phosphate. *Anal. Chim. Acta* **1995**, *302* (1), 69−74.
(24) Camargo, O. A.; Moniz, A. C.; Jorge, J. A.; Valadares, J. M. A. S. *Métodos de análise química, mineralógica e física de solos*; Instituto Agronômico de Campinas: Campinas, 2009; p 77.
(25) Kilmer, V. J.; Alexander, L. T. Methods of making mechanical analyses of soils. *Soil Sci.* **1949**, *68* (1), 15−24.
(26) Empresa Brasileira de Pesquisa Agropecuária. *Manual de métodos de análise de solo*; Embrapa Solos: Rio de Janeiro, 1979; p 247.
(27) Nelson, D. W.; Sommers, L. E. *Total carbon, organic carbon, and organic matter*; SSSA and ASA: Madison, 1996; pp 961−1010.
(28) Gatiboni, L. C. *Disponibilidade de formas de fosforo no solo às plantas*; Universidade Federal de Santa Maria: Santa Maria, RS, 2003.
(29) Ravel, B.; Newville, M. ATHENA, ARTEMIS, HEPHAESTUS: data analysis for X-ray absorption spectroscopy using IFEFFIT. *J. Synchrotron Radiat.* **2005**, *12*, 537−541.
(30) Luo, L.; Ma, Y. B.; Sanders, R. L.; Xu, C.; Li, J. M.; Myneni, S. C. B. Phosphorus speciation and transformation in long-term fertilized soil: evidence from chemical fractionation and P K-edge XANES spectroscopy. *Nutr. Cycling Agroecosyst.* **2017**, *107*, 215−226.
(31) Hashimoto, Y.; Watanabe, Y. Combined applications of chemical fractionation, solution P-31-NMR and P K-edge XANES to determine phosphorus speciation in soils formed on serpentine landscapes. *Geoderma* **2014**, *230-231*, 143−150.
(32) Eriksson, A. K.; Gustafsson, J. P.; Hesterberg, D. Phosphorus speciation of clay fractions from long-term fertility experiments in Sweden. *Geoderma* **2015**, *241-242*, 68−74.
(33) Liu, J.; Yang, J. J.; Cade-Menun, B. J.; Hu, Y. F.; Li, J. M.; Peng, C.; Ma, Y. B. Molecular speciation and transformation of soil legacy phosphorus with and without long-term phosphorus fertilization: Insights from bulk and microprobe spectroscopy. *Sci. Rep.* **2017**, *7*, 12.
(34) Wisawapipat, W.; Charoensri, K.; Runglerttrakoolchai, J. Solid-phase speciation and solubility of phosphorus in an acid sulfate paddy soil during soil reduction and reoxidation as affected by oil palm ash and biochar. *J. Agric. Food Chem.* **2017**, *65* (4), 704−710.
(35) Hesterberg, D.; Zhou, W. Q.; Hutchison, K. J.; Beauchemin, S.; Sayers, D. E. XAFS study of adsorbed and mineral forms of phosphate. *J. Synchrotron Radiat.* **1999**, *6*, 636−638.

DOI: 10.1021/acssuschemeng.8b02511
ACS Sustainable Chem. Eng. 2018, 6, 12187−12196

(36) Ajiboye, B.; Akinremi, O. O.; Jurgensen, A. Experimental validation of quantitative XANES analysis for phosphorus speciation. *Soil Sci. Soc. Am. J.* **2007**, *71* (4), 1288−1291.
(37) Werner, F.; Prietzel, J. Standard Protocol and Quality Assessment of Soil Phosphorus Speciation by P K-Edge XANES Spectroscopy. *Environ. Sci. Technol.* **2015**, *49* (17), 10521−10528.
(38) Li, Z.; Bai, T. S.; Dai, L. T.; Wang, F. W.; Tao, J. J.; Meng, S. T.; Hu, Y. X.; Wang, S. M.; Hu, S. J. A study of organic acid production in contrasts between two phosphate solubilizing fungi: Penicillium oxalicum and Aspergillus niger. *Sci. Rep.* **2016**, *6*, 8.
(39) de Oliveira Mendes, G.; Moreira de Freitas, A. L.; Liparini Pereira, O.; Ribeiro da Silva, I.; Bojkov Vassilev, N.; Dutra Costa, M. Mechanisms of phosphate solubilization by fungal isolates when exposed to different P sources. *Ann. Microbiol.* **2014**, *64* (1), 239−249.
(40) Talbot, D.; Talbot, J. *Corrosion Science and Technology*; Materials Science & Technology; CRC Press LLC: Boca Raton, FL, 1997; p 390.

DOI: 10.1021/acssuschemeng.8b02511
ACS Sustainable Chem. Eng. 2018, 6, 12187−12196